Development 138, 2079-2088 (2011) doi:10.1242/dev.059808

Primary cilia control telencephalic patterning and morphogenesis via Gli3 proteolytic processing

Laurianne Besse[1,2,3], Mariame Neti[1,2,3], Isabelle Anselme[1,2,3], Christoph Gerhardt[4], Ulrich Rüther[4], Christine Laclef[1,2,3,*] and Sylvie Schneider-Maunoury[1,2,3,*,†]

SUMMARY

Primary cilia have essential functions in vertebrate development and signaling. However, little is known about cilia function in brain morphogenesis, a process that is severely affected in human ciliopathies. Here, we study telencephalic morphogenesis in a mouse mutant for the ciliopathy gene *Ftm* (*Rpgrip1l*). We show that the olfactory bulbs are present in an ectopic location in the telencephalon of $Ftm^{-/-}$ fetuses and do not display morphological outgrowth at the end of gestation. Investigating the developmental origin of this defect, we have established that E12.5 $Ftm^{-/-}$ telencephalic neuroepithelial cells lack primary cilia. Moreover, in the anterior telencephalon, the subpallium is expanded at the expense of the pallium, a phenotype reminiscent of *Gli3* mutants. This phenotype indeed correlates with a decreased production of the short form of the Gli3 protein. Introduction of a *Gli3* mutant allele encoding the short form of Gli3 into *Ftm* mutants rescues both telencephalic patterning and olfactory bulb morphogenesis, despite the persistence of cilia defects. Together, our results show that olfactory bulb morphogenesis depends on primary cilia and that the essential role of cilia in this process is to produce processed Gli3R required for developmental patterning. Our analysis thus provides the first in vivo demonstration that primary cilia control a developmental process via production of the short, repressor form of Gli3. Moreover, our findings shed light on the developmental origin of olfactory bulb agenesis and of other brain morphogenetic defects found in human diseases affecting the primary cilium.

KEY WORDS: Primary cilium, *Ftm* (*Rpgrip1l*), Gli3, Telencephalon, Olfactory bulb, Mouse

INTRODUCTION

During vertebrate development, the brain becomes progressively subdivided into distinct regions with specific properties of cell specification, growth and morphogenesis. Telencephalic patterning relies on three main signaling centers: the anterior neural ridge (ANR), the ventral telencephalon and the dorsal telencephalic midline, which produce fibroblast growth factors (FGFs), sonic hedgehog (Shh) and Wnts/bone morphogenetic proteins (BMPs), respectively. These signaling centers interact with each other and set up a complex regulatory hierarchy of transcription factors (Hebert and Fishell, 2008). The zinc-finger transcription factor Gli3 plays a crucial role in telencephalic patterning (Aoto et al., 2002). The mouse *extra-toes* mutant (Xt^J, hereafter $Gli3^{Xt}$), which behaves as a null *Gli3* mutant (Büscher and Rüther, 1998), has a severely reduced dorsomedial telencephalon and lacks olfactory bulbs (OBs) (Hui and Joyner, 1993). Instead, it presents an expanded subpallium, in particular in the most anterior region (Theil et al., 1999; Tole et al., 2000; Aoto et al., 2002; Kuschel et al., 2003). In addition, some $Gli3^{Xt/Xt}$ embryos are exencephalic. Gli3 is an effector of the Hh pathway in vertebrates. In the absence of Hh ligand, Gli3 is cleaved in a ubiquitin/proteasome-dependent process into a short form (Gli3-83) with transcriptional repressor activity (Gli3R) (Wang et al., 2000; Tempe et al., 2006). In the presence of Hh, the cleavage of Gli3 is inhibited and a full-length (Gli3-190) transcriptional activator form (Gli3A) is produced (Bai et al., 2004).

Recently, Gli3 functions were shown to depend on primary cilia (Haycraft et al., 2005; Huangfu and Anderson, 2005; Liu et al., 2005; May et al., 2005; Eggenschwiler and Anderson, 2007). Primary cilia are present on almost every cell during vertebrate embryogenesis. They consist of a specialized plasma membrane supported by a specific microtubule network, the axoneme, anchored to the basal body (Marshall, 2008; Gerdes et al., 2009). Ciliogenesis and cilia function rely on a process called intraflagellar transport (IFT), which involves molecular motors and IFT protein complexes (Rosenbaum and Witman, 2002). The study of IFT gene mouse mutants has revealed important functions for vertebrate primary cilia in signal transduction (Rosenbaum and Witman, 2002; Gerdes and Katsanis, 2008; Wong and Reiter, 2008; Neugebauer et al., 2009). In particular, IFT mutants display neural tube patterning defects and polydactyly, resulting from perturbations in the Hh signaling pathway. Both genetic and in vitro studies have shown an essential role for cilia, downstream of the patched 1 (Ptc1, or Ptch1) receptor and smoothened (Smo) co-receptor, in the formation of the full activator forms of Gli2 and Gli3. Interestingly, mouse mutants for a number of genes involved in anterograde and retrograde IFT and, more generally, in cilia maintenance, show an increased Gli3-190:Gli3-83 ratio. This observation has led to the proposal that cilia are also required for the production of a short, repressor form of Gli3 in the absence of Hh signaling (Haycraft et al., 2005; Huangfu and Anderson, 2005; Liu et al., 2005; May et al., 2005; Huangfu and Anderson, 2006; Eggenschwiler and Anderson, 2007; Hoover et al., 2008; Tran et al., 2008; Cortellino et al., 2009). However, the demonstration that important aspects of cilia function are mediated by the control of Gli3R production has yet to be provided in vivo. The mouse telencephalon is an ideal structure with which to test

[1]CNRS UMR 7622, 9 Quai Saint Bernard, Boîte 24, F-75005, Paris, France. [2]UPMC Université Paris 06 UMR 7622, 9 Quai Saint Bernard, Boîte 24, F-75005, Paris, France. [3]INSERM U969, 9 Quai Saint Bernard, Boîte 24, F-75005, Paris, France. [4]Institut für Entwicklungs und Molekularbiologie der Tiere (EMT), Heinrich-Heine-Universität, 40225 Düsseldorf, Germany.

*These authors contributed equally to this work
†Author for correspondence (sylvie.schneider-maunoury@snv.jussieu.fr)

Accepted 23 February 2011

this hypothesis, given that *Gli3* is a central effector in telencephalic patterning and acts mainly as a repressor in this structure (Rallu et al., 2002).

Consistent with the broad distribution and multiple functions of cilia, a large group of human diseases has been linked to primary cilium dysfunction. These pleiotropic and genetically heterogeneous diseases have been collectively termed ciliopathies (Badano et al., 2006; Sharma et al., 2008). We and others recently reported mutations in the human *Ftm* orthologue *RPGRIP1L* in Meckel (MKS; OMIM #611561) and Joubert type B (OMIM #611560) syndromes, which are autosomal recessive multisystem ciliopathies (Arts et al., 2007; Delous et al., 2007). The Ftm protein is widely expressed during embryogenesis, is mainly found at the base of primary cilia and is required for normal ciliogenesis in the mouse node, limb buds and spinal cord (Arts et al., 2007; Delous et al., 2007; Vierkotten et al., 2007). Mice with a targeted inactivation of the *Ftm* gene die around birth and recapitulate most malformations observed in MKS fetuses, including exencephaly, polydactyly and kidney cysts (Delous et al., 2007; Vierkotten et al., 2007). In the spinal cord of $Ftm^{-/-}$ embryos, a loss of the floor plate and a strong reduction in motoneuron and V3 interneuron progenitors point to reduced Hh signaling (Vierkotten et al., 2007). Accordingly, genetic and in vitro evidence suggests that *Ftm*, similar to IFT genes, interacts with the Hh pathway downstream of Smo and upstream of Gli2 and Gli3.

In this study, we analyze the role of *Ftm* in telencephalic patterning and morphogenesis. We show that non-exencephalic $Ftm^{-/-}$ fetuses display a mislocalized OB-like (OBL) structure, which does not show morphological outgrowth. We next investigate the developmental origin of this defect in the telencephalon of E12.5 $Ftm^{-/-}$ embryos and observe that most telencephalic neuroepithelial cells lack normal primary cilia. Furthermore, in these mutant embryos, the subpallium is expanded at the expense of the pallium, a phenotype reminiscent of *Gli3* mutant mice, and the Gli3-190:Gli3-83 ratio is increased. Interestingly, the introduction of one or two alleles of $Gli3^{\Delta 699}$, which produces only a short form of Gli3 (Böse et al., 2002), into the $Ftm^{-/-}$ background leads to the rescue of telencephalic patterning and OB morphogenesis, whereas cilia are not restored. Our work thus provides the first functional evidence that *Ftm* and cilia are essential for OB morphogenesis and that their function in this process is mediated by the control of Gli3R production.

MATERIALS AND METHODS

Mouse strains

Ftm, $Gli3^{Xt}$, $Gli3^{Pdn}$ and $Gli3^{\Delta 699}$ mutant mice were maintained in a C57Bl6/J background. Double heterozygous $Ftm^{+/-}$ $Gli3^{+/\Delta 699}$ mice were obtained and incrossed in order to study the phenotype of compound mutant fetuses. PCR genotyping was performed as previously described (Büscher and Rüther, 1998; Böse et al., 2002; Kuschel et al., 2003; Vierkotten et al., 2007). Embryonic day (E) 0.5 was defined as noon on the day of vaginal plug detection.

In situ hybridization, immunofluorescence and EdU staining

For histology and in situ hybridization (ISH), embryos were dissected in cold phosphate-buffered saline (PBS) and fixed overnight in 60% ethanol, 30% formaldehyde and 10% acetic acid. Embryos were embedded in paraffin and sectioned (8 μm). Cresyl thionin staining and ISH were performed as previously described (Anselme et al., 2007). For immunofluorescence, fetuses were perfused with 4% paraformaldehyde. Immunofluorescence stainings were performed on 14 μm serial cryostat sections as described (Anselme et al., 2007), with antibodies against Arl13b (Caspary et al., 2007), acetylated tubulin (Sigma), GABA (Sigma), γ-tubulin (Sigma), Pax6 (Covance), Tbr1 (Chemicon), Tbr2 (Chemicon), Omp (Wako) and tyrosine hydroxylase (Chemicon). Nuclei were counterstained with DAPI. For S-phase cell detection, intraperitoneal injections of pregnant mice were performed with 100-200 μg 5-ethynyl-2′-deoxyuridine (EdU) in PBS and embryos were harvested 1 hour later (Salic and Mitchison, 2008). Anti-EdU staining was performed according to the manufacturer's recommendations (Click-iT EdU Alexa Fluor Imaging Kit, Invitrogen).

Scanning electron microscopy

Embryos were dissected in 1.22× PBS (pH 7.4) and fixed overnight with 2% glutaraldehyde in 0.61× PBS (pH 7.4) at 4°C. Heads were then sectioned to separate the dorsal and ventral parts of the telencephalon, exposing their ventricular surfaces. Head samples were washed several times in 1.22× PBS and postfixed for 15 minutes in 1.22× PBS containing 1% OsO4. Fixed samples were washed several times in ultrapure water, dehydrated with a graded series of ethanol and prepared for scanning electron microscopy using the critical point procedure (CPD7501, Polaron). Their surfaces were coated with a 20 nm gold layer using a gold spattering device (Scancoat Six, Edwards). Samples were observed under a Cambridge S260 scanning electron microscope at 10 keV.

Transmission electron microscopy

Tissues were fixed for 1 hour with 3% glutaraldehyde, post-fixed in 1.22× PBS containing 1% OsO4, then dehydrated with a graded ethanol series. After 10 minutes in a 1:2 mixture of propane:epoxy resin, tissues were embedded in gelatin capsules with freshly prepared epoxy resin and polymerized at 60°C for 24 hours. Sections (80 nm) obtained using an ultramicrotome (Reichert Ultracut S) were stained with uranyl acetate and Reynold's lead citrate and observed with a Philips CM10 transmission electron microscope.

Western blotting and quantitative real-time RT-PCR

For western blots, dissected E12.5 telencephalons were frozen in liquid nitrogen and pooled as three or four of the same genotype. Protein extraction and immunoblot were performed as described (Wang et al., 2000) using mouse 6F5 anti-Gli3 (Genentech; 1:500) or mouse anti-actin (Sigma; 1:3000) antibodies.

For RT-PCR, whole RNA was extracted from dissected E12.5 telencephalons using Trizol (Invitrogen) and reverse transcribed. Quantitative real-time PCR was performed using LightCycler 480 SYBR Green I Master (Roche) and the following primers (5′ to 3′): *Gli3* (CCTGCATTGAGCTTCACCTA and TAAGCTTTGCTGTCGGCTTA) and *Ptc1* (GACCTGCTCTCCCAGTTCTC and TGCAAACGA-AGAGAGTGTCC); *Gapdh* (GGTCCTCAGTGTAGCCCAAG and AATGTGTCCGTCGTGGATCT) was used to normalize results. Each individual reaction was performed in triplicate. Statistical analysis was performed as previously described (Willaredt et al., 2008). Statistical significance was evaluated by applying Student's *t*-test to the individual relative expression values from five or six independent experiments.

RESULTS

Ftm is required for ciliogenesis in the telencephalon

The Ftm protein is present at the apical side of E12.5 telencephalic neuroepithelial cells, as a single dot distal to the basal body in control (Fig. 1A,C,D) but not $Ftm^{-/-}$ (Fig. 1B) mouse embryos. We investigated whether cilia were affected in the developing brain of $Ftm^{-/-}$ embryos. Staining with an antibody against the ciliary protein Arl13b (Caspary et al., 2007) showed the presence of cilia at the apical surface of control but not $Ftm^{-/-}$ brains (Fig. 2A,B). To confirm this observation, we used scanning electron microscopy to observe the cilia protruding into the telencephalic ventricles. In control embryos (n=11), almost all neuroepithelial cells had a single primary cilium, ~1 μm long (Fig. 2C-F). By contrast, in $Ftm^{-/-}$ embryos (n=6), most cells displayed an abnormal, short and bloated cilium-like protrusion (Fig. 2G-J). Transmission electron microscopy (Fig. 2K-T) confirmed the defect in cilium formation:

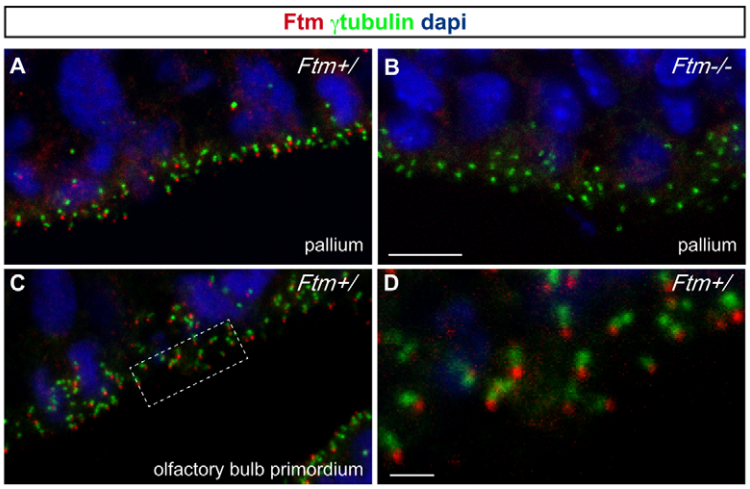

Fig. 1. Ftm localizes at the cilium base in the telencephalon of E12.5 embryos. (**A-D**) Double immunofluorescence with antibodies for Ftm (red) and γ-tubulin (green) on parasagittal sections of the telencephalon of E12.5 control (A,C,D) and *Ftm*$^{-/-}$ (B) mouse embryos, in the pallium (A,B) and olfactory bulb primordium (C,D). D is a higher magnification of the boxed region in C, highlighting Ftm localization distal to the basal body. Nuclei are counterstained with DAPI. Scale bars: 10 μm in A-C; 2 μm in D.

the protrusions were devoid of axoneme (Fig. 2P-R). By contrast, basal bodies seemed unaffected and were docked to the apical membrane in *Ftm*$^{-/-}$ (*n*=3) as in control (*n*=3) embryos (Fig. 2K,L,P-R), and the normal appearance of tight junctions suggested that the apicobasal polarity of the neuroepithelial cells was not severely perturbed (Fig. 2O,T). These observations indicate that the Ftm protein is required for cilium formation in telencephalic neuroepithelial cells.

An olfactory bulb-like structure forms in *Ftm*$^{-/-}$ fetuses

Ftm$^{-/-}$ fetuses display severe brain abnormalities, including exencephaly, reduced dorsomedial telencephalic structures and OB agenesis (Delous et al., 2007). In the present study, 60% of *Ftm*$^{-/-}$ fetuses were not exencephalic and all showed bilateral OB agenesis (*n*=84) (Fig. 3A). We investigated whether this agenesis reflected an absence of OB cell type specification. The OB has a laminar structure and is composed of two main neuronal types: projection neurons (mitral and tufted cells) and local interneurons (Long et al., 2003). At E18.5, the T-box transcription factor Tbr2 (Eomes – Mouse Genome Informatics) is present at high levels in differentiated OB projection neurons (Fig. 3C,E) and, at a lower level, in OB interneurons in the granular layer and in cortical neuronal progenitors undergoing radial migration and differentiation (Englund et al., 2005; Brill et al., 2009). We found that the pallium of *Ftm*$^{-/-}$ fetuses contained an ectopic group of Tbr2-positive cells, distinct from the cortical progenitors (Fig. 3D,F). In this group, many Tbr2-positive cells had a large and round nucleus, a feature characteristic of mitral cells (Fig. 3E,F, insets). However, these cells were localized more dorsally and laterally than in control embryos, and were not properly laminated (Fig. 3D,F). The presence of mitral cells in this ectopic location was confirmed by in situ hybridization (ISH) on brain sagittal sections for *Tbx21*, a T-box transcription factor gene that is expressed specifically in these cells (Fig. 3G,H) (Faedo et al., 2002). We named this ectopic site of mitral cell differentiation an OB-like (OBL) structure (Fig. 3B), in reference to a similar structure described in *Pax6* (*small eye*, *Sey*) mutant mice (Jimenez et al., 2000). In this ectopic structure, we assessed the presence of OB interneurons, which are born in the dorsal part of the lateral ganglionic eminence (dLGE) and migrate towards the OB via the rostral migratory stream. Both γ-amino butyric acid (GABA)-positive and tyrosine hydroxylase (Th)-positive interneurons were present in the OBL and were not properly laminated, as with the projection neurons (Fig. 3I-L).

Our study of OB cell types at the end of gestation thus shows that OB agenesis in *Ftm*$^{-/-}$ fetuses does not result from a cell specification defect, but from abnormal morphogenesis, possibly linked to the aberrant localization of the OBL.

Ftm$^{-/-}$ olfactory sensory neurons differentiate but do not contact mitral cells

OB lamination and outgrowth depend on the arrival of olfactory sensory neuron (OSN) axons (Gong and Shipley, 1995; Hirata et al., 2006). OSNs differentiate in the olfactory epithelium (OE). Their axons enter the anterior telencephalon at ~E11.5 in the mouse, and then make contacts with mitral cell dendrites in glomeruli (Whitesides and LaMantia, 1996; Blanchart et al., 2006). We analyzed both cell differentiation in the OE and the trajectories of OSN axons in *Ftm* mutants. Differentiated OSNs were present in the OE of *Ftm*$^{-/-}$ fetuses (data not shown) and OSN axons positive for the olfactory marker protein (Omp) reached the ventral telencephalon in *Ftm*$^{-/-}$ as well as in control fetuses (Fig. 3M-O). However, instead of invading the OB as in controls (Fig. 3M), the mutant OSN axons remained together close to the ventral telencephalon (Fig. 3O) and did not enter the ectopic OBL (Fig. 3N). This lack of connection between OSN axons and mitral cells might contribute to the absence of OBL lamination and outgrowth.

The OB primordium is specified in an ectopic position in the telencephalon of *Ftm*$^{-/-}$ embryos

In order to trace back the origin of OB agenesis, we investigated earlier stages of telencephalic development. The OB primordia (OBp) originate in the anterior part of the ventral pallium (Cobos et al., 2001; Marin and Rubenstein, 2003). At E13.5 the OBp are morphologically distinguishable as anterior buddings of the neuroepithelium in each telencephalic hemisphere, and express the transcription factor genes *Er81* and *AP2e* (*Etv1* and *Tcfap2e* – Mouse Genome Informatics) (Fig. 4A,C) (Fukuchi-Shimogori and Grove, 2003; Stenman et al., 2003; Feng et al., 2009). In E13.5 *Ftm*$^{-/-}$ embryos, we observed *Er81*- and *AP2e*-expressing cells in a dorsolateral domain of the telencephalon, although we could not detect any budding of the OBp (Fig. 4B,D). This shows that the OBp is specified in an aberrant position and that OB initial outgrowth is impaired in *Ftm*$^{-/-}$ embryos. As OB budding correlates with a sudden reduction in the rate of cell proliferation in the OBp ventricular zone (Gong and Shipley, 1995; Hebert et al., 2003), we analyzed cell proliferation in E12.5 *Ftm*$^{-/-}$ embryos. By counting the proportion of neuroepithelial cells in S phase in

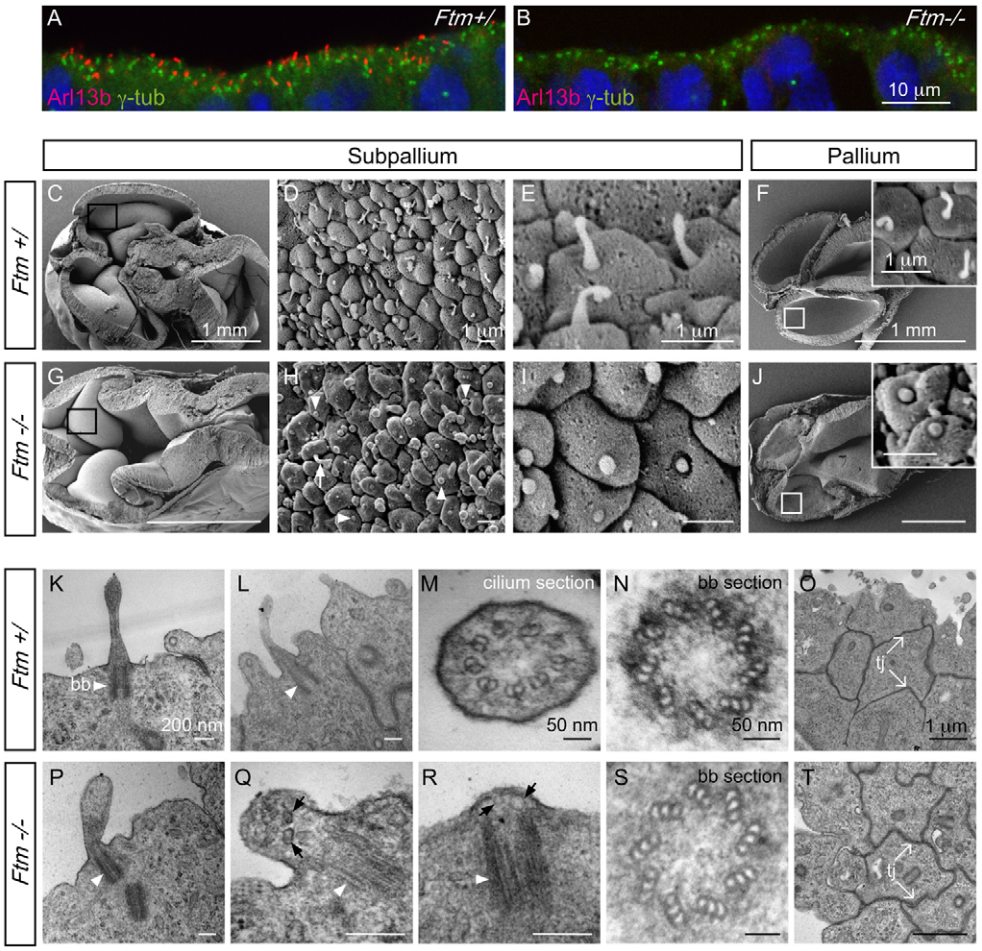

Fig. 2. Impaired ciliogenesis in the telencephalon of *Ftm*$^{-/-}$ embryos. (**A**,**B**) Immunofluorescence on telencephalic sections of control (labeled *Ftm*$^{+/}$ for *Ftm*$^{+/+}$ or *Ftm*$^{+/-}$) (A) and *Ftm*$^{-/-}$ (B) mouse embryos with antibodies to Arl13b (cilium) and γ-tubulin (basal body). Nuclei are counterstained with DAPI (blue). (**C-J**) Scanning electron microscopy of the ventricular surface of the subpallium (C-E,G-I) and pallium (F,J) of control (C-F) and *Ftm*$^{-/-}$ (G-J) E12.5 embryos. In H, the arrowheads point to rounded and short cilia and the arrow points to a normal cilium. (**K-T**) Ultrastructure of telencephalic neuroepithelial cells and primary cilia by transmission electron microscopy of control (K-O) and *Ftm*$^{-/-}$ (P-T) E12.5 embryos. (K,L,P-R) Longitudinal sections through cilia; white arrowheads point to basal bodies (bb). Black arrows (Q,R) point to small vesicles in a ciliary compartment in *Ftm*$^{-/-}$ embryos. (M) Transverse section through the axoneme of a primary cilium. (N,S) Transverse sections through basal bodies. tj, tight junction. Scale bars: 1 mm in C,F,G,J; 10 μm in A,B; 1 μm in D,E,H,I,O,T and insets in F,J; 200 nm in K,P-R; 50 nm in L-N,S.

different telencephalic domains by EdU incorporation, we found that the proportion of EdU-positive cells in *Ftm*$^{-/-}$ embryos was similar in the cortex and in the *Er81*-positive region (the OBL), in contrast to control siblings (Fig. 4E). Thus, although the OBp is present in the *Ftm*$^{-/-}$ telencephalon, its specific cell cycle properties are impaired.

Ventral structures are expanded dorsally in the anterior telencephalon of *Ftm*$^{-/-}$ embryos

The dorsolateral position of the OBp in E12.5 *Ftm*$^{-/-}$ embryos could suggest dorsoventral (DV) telencephalic patterning defects. In order to test this hypothesis, we analyzed the expression of *Ngn2* (*Neurog2* – Mouse Genome Informatics) and *Pax6* as dorsal markers and *Dlx2* and *Gsx2* (*Gsh2*) as ventral markers. *Dlx2* and *Ngn2* are expressed in mutually exclusive ventral (subpallial) and dorsal (pallial) domains and present a common limit at the pallial-subpallial boundary, whereas *Pax6* and *Gsx2* expression domains overlap in the dorsal subpallium (the dLGE) (Yun et al., 2001). The parasagittal section plane we used allowed us to analyze their relationships in the most anterior telencephalon. In control embryos, *Dlx2* and *Ngn2* were expressed in mutually exclusive areas in the most anterior telencephalon (Fig. 4F,H) and the OBp formed in the dorsal *Ngn2*-positive domain, just above this gene expression boundary (Fig. 4A,C,F,H). The anterior expression limit of *Gsx2* was similar to that of *Dlx2* (Fig. 4H,L), and the *Pax6* domain partially overlapped with that of *Gsx2* and *Dlx2* (Fig. 4H,J,L). In *Ftm*$^{-/-}$ embryos, dorsal *Ngn2* and *Pax6* expression was markedly reduced in the anterior telencephalon (Fig. 4G,K), whereas the *Dlx2* and *Gsx2* expression domains were expanded anteriorly and dorsally to span the most anterior telencephalon (Fig. 4I,M). Interestingly, *Er81*-expressing cells were located in the *Ngn2*-positive dorsal domain, just above the ectopic *Ngn2/Dlx2* boundary (Fig. 4B,D,G,I). The analysis of E14.5 telencephalic coronal sections confirmed the dorsal expansion of ventral structures in the anterior *Ftm*$^{-/-}$ telencephalon and revealed milder defects in more caudal regions of the telencephalon, where the pallial-subpallial boundary was less distinct in *Ftm*$^{-/-}$ than in control fetuses (see Fig. S1 in the supplementary material). Thus, the dorsal expansion of ventral structures is limited to the most anterior part of the telencephalon. A similar, although milder, patterning defect was observed in the anterior telencephalon of E10.5 *Ftm*$^{-/-}$ embryos (see Fig. S2 in the supplementary material).

Taken together, our data point to a dorsal expansion of ventral structures in the anterior telencephalon of *Ftm* mutants, and strongly suggest that the aberrant localization of the OBp results from this DV patterning defect. This phenotype is reminiscent of that of *Gli3*^{Xt} and *Gli3*^{Pdn} mutants, in which *Dlx2* expression is expanded dorsally in the anterior telencephalon at E12.5 (Kuschel et al., 2003). Notably, *Gli3*^{Xt} mutants lack OBs (Johnson, 1967; Balmer and LaMantia, 2004). We compared the *Gli3* and *Ftm* mutant phenotypes in greater detail and found that both *Gli3*$^{Xt/Xt}$ and *Gli3*$^{Pdn/Pdn}$ embryos had an ectopic, more dorsal OBp in the E13.5 telencephalon and that the anterior *Ngn2/Dlx2* boundary was shifted dorsally in both mutants (see Fig. S3 in the supplementary material). The phenotype of the *Gli3*$^{Pdn/Pdn}$ telencephalon was very similar to that of *Ftm*$^{-/-}$, whereas *Gli3*$^{Xt/Xt}$ embryos were more

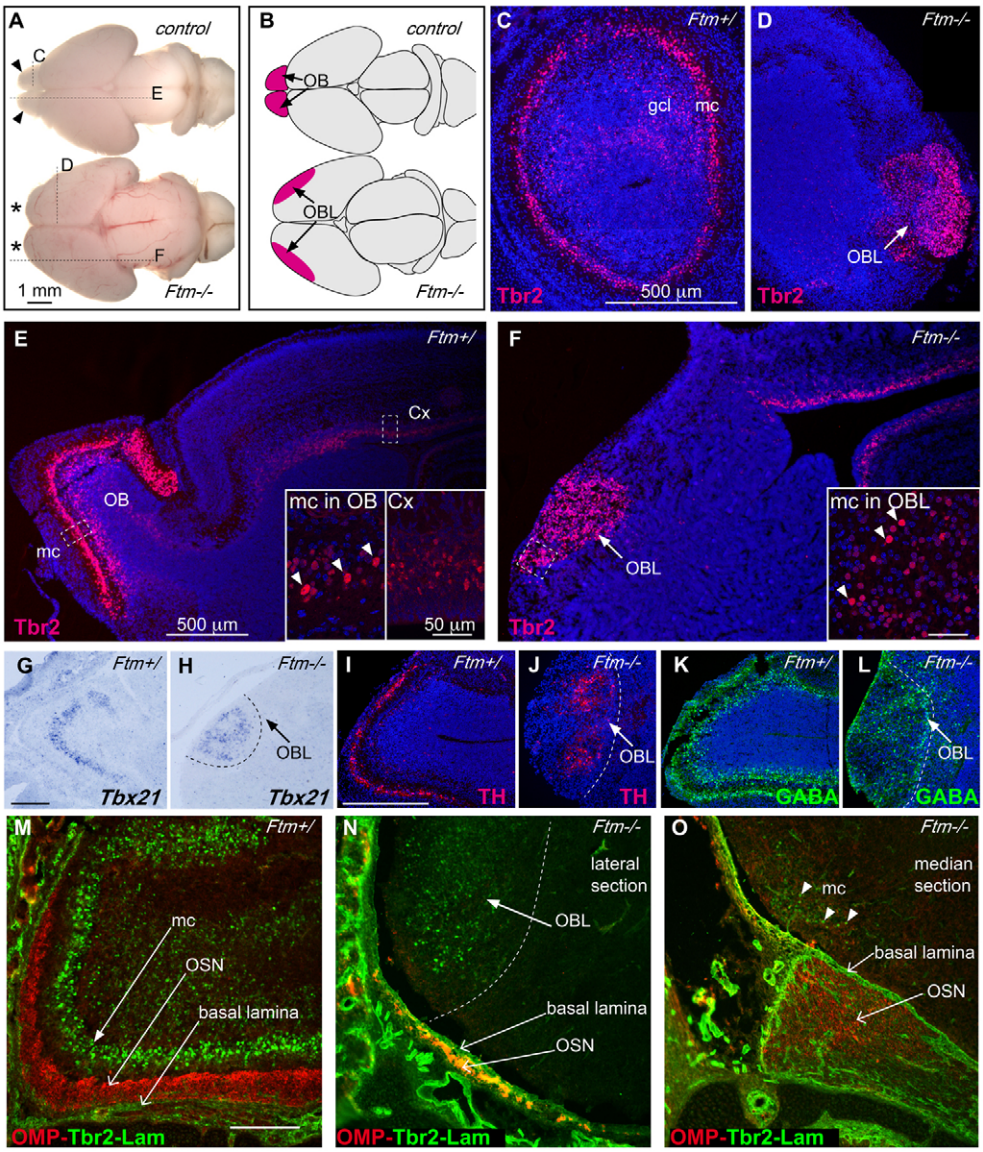

Fig. 3. The *Ftm*$^{-/-}$ telencephalon contains a mislocalized olfactory bulb-like structure. (**A**) Dissected brains of E18.5 control (top) and *Ftm*$^{-/-}$ (bottom) mouse fetuses. The olfactory bulbs (OBs) are conspicuous in control (arrowheads) but not in *Ftm*$^{-/-}$ (asterisks) brain. Vertical and horizontal dashed lines indicate the position of coronal and sagittal sections shown in C,D and E,F, respectively. (**B**) Schematic showing the localization of the OB-like (OBL) structure. (**C-H**) Tbr2 immunofluorescence (C,D) and in situ hybridization (ISH) with a *Tbx21* probe (G,H) show ectopic mitral cells in the lateral pallium. mc, mitral cell layer; gcl, granule cell layer; Cx, differentiating cortical neurons. Insets in E show the large, round nuclei of mitral cells in the OB (left, mc in OB, arrowheads) as compared with the smaller nuclei of Tbr2-positive cells in the cortex (right, Cx). Inset in F shows the large and round nuclei of Tbr2-positive cells in the OBL of *Ftm*$^{-/-}$ fetuses (mc in OBL, arrowheads). (**I-L**) Immunodetection of tyrosine hydroxylase (Th) and γ-amino butyric acid (GABA) shows the presence of mature periglomerular interneurons in the OB of control (I,K) and their disorganization in the OBL of *Ftm*$^{-/-}$ fetuses (J,L). (**M-O**) Immunodetection of the olfactory marker protein (Omp, red), Tbr2 (green) and laminin (green) in parasagittal telencephalic sections of control (M) and *Ftm*$^{-/-}$ (N,O) fetuses. N is a lateral section (OBL level) and O is a more medial section. The dashed line marks the boundary of the OBL. Scale bars: 1 mm in A; 500 µm in C-F and I-L; 50 µm in insets in E,F; 200 µm in G,H,M-O.

severely affected. Nevertheless, an OBL was present in the E18.5 *Gli3*$^{Xt/Xt}$ dorsal telencephalon (see Fig. S3 in the supplementary material).

Gli3 processing and function are impaired in the *Ftm*$^{-/-}$ telencephalon

The similarity between *Ftm*$^{-/-}$ and *Gli3*$^{Pdn/Pdn}$ telencephalic phenotypes suggests that the absence of Ftm could lead to decreased *Gli3* expression levels and/or impaired Gli3 protein activity in the telencephalon. Neither RT-PCR nor ISH on E12.5 coronal sections detected any significant change in *Gli3* mRNA levels in *Ftm*$^{-/-}$ telencephalon as compared with control littermates (Fig. 5A-C). Thus, the DV patterning defect is not caused by a reduction in *Gli3* expression levels.

An altered Gli3-190:Gli3-83 ratio has been described in a number of IFT mutant mice (Haycraft et al., 2005; Liu et al., 2005; May et al., 2005). Consistent with the IFT-like phenotype of *Ftm* mutants, an increased Gli3-190:Gli3-83 ratio was described for E11.5 *Ftm*$^{-/-}$ whole embryos (Vierkotten et al., 2007). Since cilium function may have different effects on Gli transcription factors depending on the tissue and stage (Huangfu and Anderson, 2005; Eggenschwiler and Anderson, 2007), we examined the Gli3-190:Gli3-83 ratio by western blot on E12.5 telencephalic extracts (Fig. 5D). In control telencephalic extracts, Gli3-83 was 5-fold more abundant than Gli3-190 (Fig. 5D,E). In the telencephalon of *Ftm*$^{-/-}$ embryos, although the total amount of Gli3 protein was similar to that in the control, the level of Gli3-190 was elevated and Gli3-83 was lowered, leading to an inverted ratio, with Gli3-190 being 8.5-fold more abundant than Gli3-83 (Fig. 5D,E). This reduction in the abundance of Gli3-83 correlated with a reduction in Gli3R activity, as dorsomedial telencephalic structures, which depend on *Gli3* for their formation (Theil et al., 1999; Tole et al., 2000; Kuschel et al., 2003), were reduced in size and were misshapen (see Fig. S4 in the supplementary material). These data demonstrate that, in the telencephalon, *Ftm* is required for the proper processing of Gli3 into its repressor form.

Both FGF signaling from the ANR and Hh signaling from the ventral telencephalon have been implicated in the specification of ventral telencephalic fates (Hebert and Fishell, 2008). Moreover, *alien* (*Ttc21b*) mutants affected in retrograde IFT display a ventralized telencephalon caused by increased Hh expression and signaling (Stottmann et al., 2009). The telencephalic phenotype of

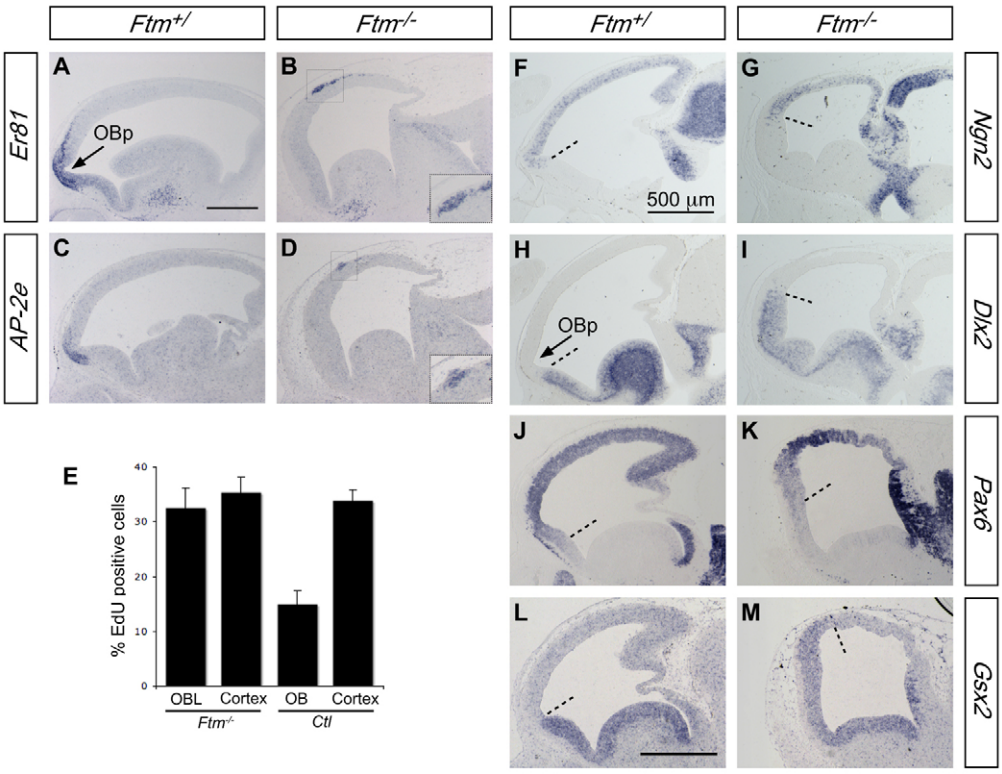

Fig. 4. OB primordium formation and telencephalic dorsoventral patterning at E12.5-E13.5. (**A-D**) ISH on parasagittal sections of E13.5 control (A,C) and *Ftm*$^{-/-}$ (B,D) mouse brains with *Er81* (A,B) and *AP2e* (C,D) probes, showing early cell differentiation in the OB primordium (OBp, arrow in A). Insets in B and D are higher magnifications of the OBp-specific cells that are present in an ectopic position in the *Ftm*$^{-/-}$ telencephalon. (**E**) Quantification of EdU incorporation, which marks cells in S phase, in different telencephalic domains: cortex versus OB or OBL regions in E12.5 control (Ctl) and *Ftm*$^{-/-}$ embryos. Error bars indicate mean relative expression values ± s.e.m. (**F-M**) ISH on parasagittal sections of E12.5 control (F,H,J,L) and *Ftm*$^{-/-}$ (G,I,K,M) embryos with *Ngn2* (F,G), *Dlx2* (H,I), *Pax6* (J,K) and *Gsx2* (L,M) probes. Dashed lines indicate the anterior boundaries of the gene expression domains. These boundaries are shifted dorsally in *Ftm*$^{-/-}$ embryos (G,I,K,M). Scale bars: 500 μm.

Ftm mutants could therefore result from increased FGF or Hh pathway activity. *Fgf8* expression and signaling from the ANR were not obviously altered in *Ftm*$^{-/-}$ embryos from E8.5 to E12.5 (see Fig. S5 in the supplementary material; data not shown). We tested Hh pathway activity by examining the expression of four target genes, *Shh*, *Gli1*, *Ptc1* and *Nkx2.1*, that are known to respond differentially to Hh signaling in the telencephalon (Rallu et al., 2002). At E9.5-E12.5, all four genes were expressed in the ventral telencephalon with distinct patterns (Fig. 5F-M; data not shown). In the E9.5 telencephalon, *Shh* and *Nkx2.1* expression was similar in *Ftm*$^{-/-}$ and controls (data not shown). At E12.5, telencephalic expression of *Shh*, *Gli1* and *Nkx2.1* was maintained or slightly reduced (Fig. 5G,I,K) and *Gli1* expression was more scattered (Fig. 5I) in *Ftm*$^{-/-}$ than in control embryos. By contrast, *Ptc1* was expanded dorsally (Fig. 5M). The upregulation of *Ptc1* expression was confirmed by quantitative RT-PCR from *Ftm*$^{-/-}$ telencephalic extracts (Fig. 5N). Interestingly, we detected a similar *Ptc1* expansion in *Gli3*$^{Xt/Xt}$ embryos (data not shown), confirming that *Ptc1* does not require Gli3A for its activation (Rallu et al., 2002).

These results argue against an increase in the Hh pathway and/or Gli3A activity in the *Ftm*$^{-/-}$ telencephalon. The dorsal expansion of the *Ptc1* expression domain and the dorsal shift of the anterior telencephalic DV boundary might therefore result from a reduction in Gli3R activity. Together, these data strongly suggest that the DV patterning defect of the *Ftm*$^{-/-}$ anterior telencephalon is due to a reduction in Gli3R production.

Gli3$^{\Delta 699}$ rescues telencephalic patterning and OB morphogenesis defects in *Ftm*$^{-/-}$ fetuses

If, as we propose, the telencephalic patterning defects in *Ftm*$^{-/-}$ embryos result from a reduction in Gli3R levels, it should be possible to rescue these defects by introducing a constitutively active repressor form of Gli3 into the *Ftm* mutant background. To test this, we used *Gli3*$^{\Delta 699}$ mice, obtained by the knock-in of a mutation identified in human Pallister-Hall syndrome into the *Gli3* locus (Böse et al., 2002). The *Gli3*$^{\Delta 699}$ allele exclusively produces a short (88 kDa) form of Gli3 (Fig. 5D) that lacks the transactivation domain (Böse et al., 2002; Hill et al., 2007). We first analyzed telencephalic development in *Gli3*$^{\Delta 699}$ mice, which had not been described previously. Telencephalic DV patterning was unaffected in E12.5 *Gli3*$^{\Delta 699/\Delta 699}$ embryos: expression of *Ngn2* (Fig. 6D) and *Dlx2* (Fig. 6G) was similar to that of control embryos (Fig. 4F,H). Moreover, in these mice, the OBp formed at the correct position, as shown by *Er81* expression, and presented normal outgrowth (compare Fig. 6A with Fig. 4A). At E18.5, the OB was formed normally, the different OB cell types were correctly specified and laminated, and OSN axons reached and entered the OB nerve layer (Fig. 7A,C,E,G,I,I′). This demonstrates that the activator form of Gli3 is dispensable for telencephalic patterning and OB morphogenesis and that the telencephalic defects described in *Gli3*$^{Xt/Xt}$ mutants result exclusively from the loss of Gli3R.

We then crossed *Ftm* mice with *Gli3*$^{\Delta 699}$ mice and analyzed telencephalic development in *Ftm*$^{-/-}$; *Gli3*$^{\Delta 699/\Delta 699}$ and *Ftm*$^{-/-}$; *Gli3*$^{\Delta 699/+}$ embryos. At E12.5, we observed complete rescue of the forebrain DV patterning defects: *Ftm*$^{-/-}$; *Gli3*$^{\Delta 699/\Delta 699}$ embryos showed the correct expression pattern of *Ngn2* (Fig. 6E), *Dlx2* (Fig. 6H) and *Er81* (Fig. 6B). Moreover, the OBp bulged out anteriorly as in control embryos, suggesting that initial OB morphogenesis was also restored. A partial rescue was observed in *Ftm*$^{-/-}$; *Gli3*$^{\Delta 699/+}$ embryos, with a slightly more dorsal position of the *Dlx2/Ngn2* boundary and of the OBp (Fig. 6C,F,I) and incomplete OBp bulging (Fig. 6C). Strikingly, primary cilia were totally absent from the telencephalon of E12.5 *Ftm*$^{-/-}$; *Gli3*$^{\Delta 699/\Delta 699}$ embryos (Fig. 6J,K).

We next analyzed in greater detail the extent of OB morphogenesis in E18.5 fetuses. We did not obtain *Ftm*$^{-/-}$; *Gli3*$^{\Delta 699/\Delta 699}$ fetuses at this stage. In contrast to *Ftm*$^{-/-}$ fetuses (Fig. 3), *Ftm*$^{-/-}$; *Gli3*$^{\Delta 699/+}$ fetuses displayed OB outgrowth in the expected rostral position (Fig. 7). This OB contained specific layers

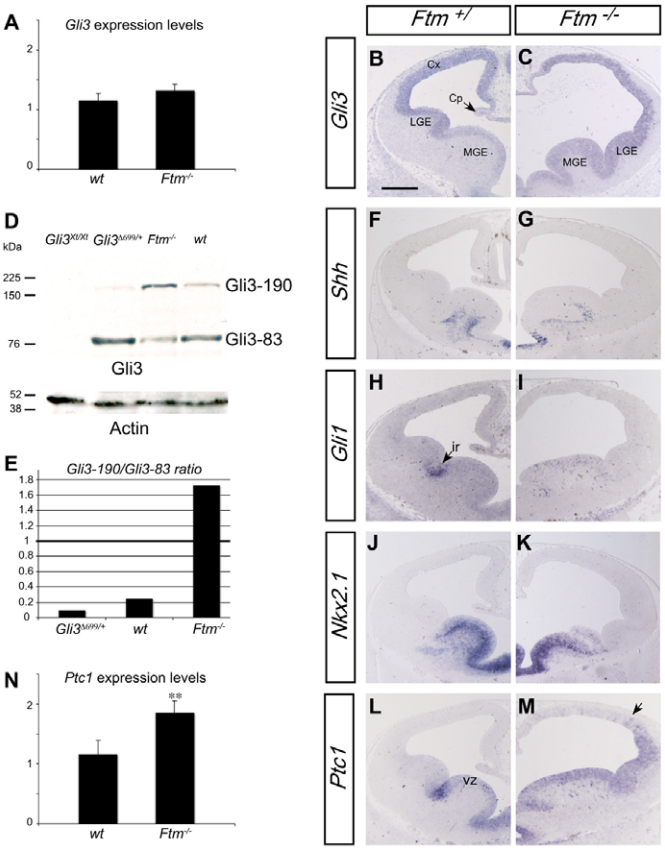

Fig. 5. Gli3 processing and activity of the Hh pathway in the telencephalon of E12.5 *Ftm*$^{-/-}$ embryos. (**A**) Quantitative RT-PCR analysis of *Gli3* expression levels in the telencephalon of E12.5 wild-type (wt) and *Ftm*$^{-/-}$ mouse embryos. (**B**,**C**) ISH with a *Gli3* probe on coronal sections of the telencephalon of *Ftm*$^{+/}$ (B) and *Ftm*$^{-/-}$ (C) embryos. (**D**) Western blot analysis of telencephalic extracts of E12.5 wild-type, *Gli3*$^{\Delta 699/+}$, *Ftm*$^{-/-}$ and *Gli3*$^{Xt/Xt}$ embryos. The *Gli3*$^{Xt/Xt}$ embryos, which do not produce Gli3 proteins, are used as a control for the specificity of the anti-Gli3 antibody. The Gli3 products at 190 kDa and 83 kDa are indicated. (**E**) Quantitation of the Gli3-190:Gli3-83 ratio in the different genetic backgrounds. (**F-M**) ISH on coronal sections of the telencephalon of *Ftm*$^{+/}$ (F,H,J,L) and *Ftm*$^{-/-}$ (G,I,K,M) embryos with probes for *Shh* (F,G), *Gli1* (H,I), *Nkx2.1* (J,K) and *Ptc1* (L,M). Cx, cortex; Cp, choroid plexus; ir, interganglionic region; LGE, lateral ganglionic eminence; MGE, medial ganglionic eminence; vz, ventricular zone. Scale bar: 300 μm. (**N**) Quantitative RT-PCR analysis of *Ptc1* expression levels in the telencephalon of E12.5 wild-type and *Ftm*$^{-/-}$ embryos. **, $P<0.001$ (Student's *t*-test). Error bars indicate mean relative expression values ± s.e.m.

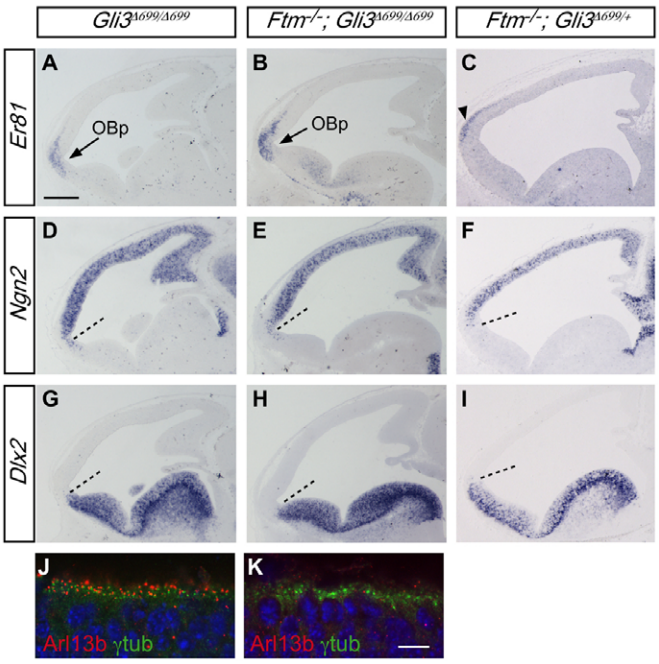

Fig. 6. Restored telencephalic patterning and OBp formation in E12.5 *Ftm*$^{-/-}$; *Gli3*$^{\Delta 699/\Delta 699}$ embryos. (**A-I**) ISH on parasagittal sections of *Gli3*$^{\Delta 699/\Delta 699}$ (A,D,G), *Ftm*$^{-/-}$; *Gli3*$^{\Delta 699/\Delta 699}$ (B,E,H) and *Ftm*$^{-/-}$; *Gli3*$^{\Delta 699/+}$ (C,F,I) mouse embryos with *Er81* (A-C), *Ngn2* (D-F) and *Dlx2* (G-I) probes. Dashed lines in D-I indicate the anterior boundary between the *Ngn2* and *Dlx2* expression domains. (**J**,**K**) Immunofluorescence with antibodies to Arl13b and γ-tubulin on E12.5 telencephalic sections of *Gli3*$^{\Delta 699/\Delta 699}$ (J) and *Ftm*$^{-/-}$; *Gli3*$^{\Delta 699/\Delta 699}$ (K) embryos. Nuclei are counterstained with DAPI (blue). Scale bars: 300 μm in A-I; 10 μm in J,K.

of projection neurons (cells positive for Tbr1, Tbr2 and Er81) (Fig. 7B,D; data not shown) and mature interneurons (cells positive for Th and GABA) (Fig. 7F,H), and Omp-positive OSN axonal termini reached and entered the OB (Fig. 7J,J′). Thus, OB outgrowth, lamination and connectivity were all partially restored by reintroduction of only one copy of *Gli3*$^{\Delta 699}$.

Our data thus demonstrate that defects in the telencephalic DV patterning and OB morphogenesis of *Ftm*$^{-/-}$ fetuses result from the reduction in Gli3R levels. Interestingly, we also observe rescue of the defects in dorsomedial telencephalon morphogenesis (see Fig. S4 in the supplementary material) and exencephaly (100% non-exencephalic embryos, n=22) in compound *Ftm*$^{-/-}$; *Gli3*$^{\Delta 699/\Delta 699}$ or *Ftm*$^{-/-}$; *Gli3*$^{\Delta 699/+}$ fetuses. By contrast, spinal cord DV patterning defects (see Fig. S6 in the supplementary material) and polydactyly (data not shown) were not rescued. Since primary cilia are not restored in the telencephalon of *Ftm*$^{-/-}$; *Gli3*$^{\Delta 699/\Delta 699}$ embryos, our data strongly suggest that the major function of primary cilia in telencephalic patterning and morphogenesis is to allow the production of Gli3R.

DISCUSSION

Ftm mutant mice are an excellent model with which to study the function of the primary cilium in telencephalic patterning and morphogenesis. Indeed, *Ftm*$^{-/-}$ fetuses display a severe phenotype that resembles that of IFT mutants and has significant similarities with human MKS, the most severe ciliopathy (Delous et al., 2007; Vierkotten et al., 2007). Moreover, a large proportion of *Ftm* homozygous mutants survive until birth, thus allowing brain morphological and anatomical analyses. In this paper, we show that OB agenesis in *Ftm* mutants originates from an early absence of OB outgrowth that is associated with DV patterning defects in the anterior telencephalon. Moreover, we demonstrate that a reduction in Gli3R levels is the sole cause of the observed telencephalic defects.

The function of cilia in the mouse spinal cord has been extensively studied, whereas only a couple of previous studies have addressed cilium function in the developing brain, and the mechanisms of OB morphogenesis have not been examined. Cilia are required after birth for Hh-dependent proliferation of granule neuron precursors in the cerebellum and dentate gyrus (Chizhikov

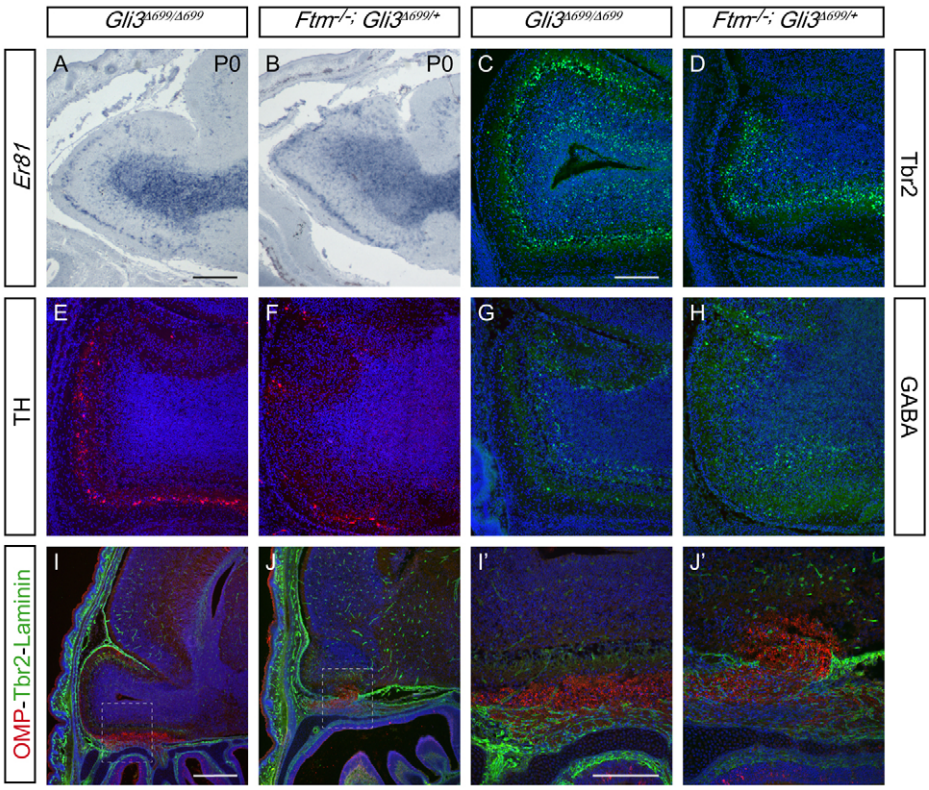

Fig. 7. The introduction of one allele of *Gli3*$^{\Delta 699}$ rescues the OB morphogenesis defects of *Ftm*$^{-/-}$ fetuses at P0. (**A**,**B**) ISH with an *Er81* probe showing the mitral cell layer and the OB interneurons in the OB of *Gli3*$^{\Delta 699/\Delta 699}$ (A) and *Ftm*$^{-/-}$; *Gli3*$^{\Delta 699/+}$ E18.5 mouse fetuses. (**C-J'**) Immunofluorescence on parasagittal sections of E18.5 *Gli3*$^{\Delta 699/\Delta 699}$ (C,E,G,I,I') and *Ftm*$^{-/-}$; *Gli3*$^{\Delta 699/+}$ (D,F,H,J,J') fetuses with antibodies for Tbr2 (C,D), Th (E,F), GABA (G,H) and Omp/Tbr2/laminin (I-J'). Scale bars: 200 μm in A-H,I',J'; 500 μm in I,J.

et al., 2007; Han et al., 2008; Spassky et al., 2008). *Ift172* null (*Slb*) mouse mutants lack telencephalic cilia and present a severe reduction in forebrain size that is attributed to an abnormal specification of the anterior mesendoderm during gastrulation (Gorivodsky et al., 2009). *Slb* mutants die at E12.5, precluding later analysis of brain morphogenesis. *Ift88* hypomorphic (*cobbletone*, *Cbs*) mouse mutants show an abnormal morphology of dorsomedial telencephalic structures with rosette-like heterotopias, and present a fuzzy pallial-subpallial boundary (Willaredt et al., 2008). This latter feature is shared by both *Dnchc2* (*Dync2h1* – Mouse Genome Informatics) mutants, which are affected in retrograde IFT (May et al., 2005), and *Ftm* mutants (present study). Interestingly, *alien* mutant mice defective in retrograde IFT show telencephalic DV patterning defects and OB agenesis similar to *Ftm* mutants, and this has been associated with enhanced Hh signaling (Stottmann et al., 2009). Contrary to *Ftm* mutants, *Cbs* and *alien* embryos display telencephalic cilia, suggesting that some ciliary functions are still present in these mice. Our results therefore advance our understanding of the role of primary cilia in the patterning and morphogenesis of the anterior telencephalon.

OB agenesis is very uncommon in mouse mutants, suggesting that OB specification and budding are controlled by robust mechanisms. Only mutants displaying a very reduced pallium, such as *Emx1/2* double knockout, *Pax6*^{Sey} and *Gli3*^{Xt} mice show OB agenesis (Johnson, 1967; Anchan et al., 1997; Dellovade et al., 1998; LaMantia, 1999; Bishop et al., 2003; Balmer and LaMantia, 2004). The similarity of the OB phenotype in *Ftm*, *Pax6*^{Sey} and *Gli3*^{Pdn} mutants suggests that it is secondary to a patterning defect. Consistently, we observed DV patterning defects in the anterior telencephalon as early as E10.5, 2 days before OB budding.

Two non-exclusive hypotheses could account for the absence of OB budding in *Ftm* mutants and its rescue by *Gli3*$^{\Delta 699}$. First, Ftm (and Gli3R) could be required within the OBp for morphogenesis. Second, the OBL could form in a region that is not permissive for budding. Conditional activation of *Ftm* in the OB will be required to discriminate between these two hypotheses. At the cellular and molecular levels, several mechanisms can be proposed to explain the OB outgrowth defect. First, the arrival of OSN axons has been proposed to be important for OB lamination and outgrowth (Gong and Shipley, 1995; Garel et al., 2003; Hebert et al., 2003; Stout and Graziadei, 1980; Gong and Shipley, 1995; Whitesides and LaMantia, 1996; Balmer and LaMantia, 2005). In *Ftm* mutants, the OSN axons are correctly targeted towards the anterior telencephalon, but very few enter the brain, similar to what had been reported for *Gli3*^{Xt} mice (St John et al., 2003; Balmer and LaMantia, 2004; Hirata et al., 2006; Watanabe et al., 2009). Thus, the absence of contact between mitral cells and OSN axons might participate in OB outgrowth defects. Second, the OB normally forms in an anterior region close to the ANR source of FGF signals and to the frontonasal mesenchymal source of retinoic acid (RA), which are both required for OB formation (Meyers et al., 1998; Garel et al., 2003; Hebert et al., 2003; Meyer and Roelink, 2003; Balmer and LaMantia, 2005). In *Ftm* mutants, the OBL forms further away from the ANR, in a region that might not receive enough of these signals. It has been proposed that a reduction in the rate of proliferation is involved in OBp outgrowth (Gong and Shipley, 1995). In *Fgfr1* mutants, the rate of cell division fails to decrease in the OBp, and this correlates with the delay in OB outgrowth (Hebert et al., 2003). Similarly, in *Ftm* mutants, we find that the proportion of S-phase nuclei fails to decrease in the OBL compared with other regions of the dorsal telencephalon. A possible explanation for the absence of OB budding might therefore be a perturbation of cell cycle kinetics linked to reduced FGF signaling in the OBp.

In *Ftm* mutant mice, opposite phenotypes are found in different regions of the central nervous system. In the spinal cord, *Ftm* mice, like many other ciliary mutants, display a reduction in ventral cell

types. Conversely, in the anterior telencephalon, we show that subpallial (ventral) markers are expanded at the expense of pallial (dorsal) markers, whereas the most ventral (*Nkx2.1*-positive) cell types appear unaffected. We cannot exclude the possibility that these differences result from regional differences in the total amount of Gli3 or in the precise Gli3A:Gli3R ratio. However, we favor an alternative hypothesis, in which region-specific responses to cilium defects result from differences in the relative importance of the activator and repressor forms of Gli2 and Gli3 along the anteroposterior axis of the neural tube. In the spinal cord, ventral cell type specification is regulated by a balance between Gli2A (and, to a lesser extent, Gli3A) and Gli3R (Ding et al., 1998; Theil et al., 1999; Park et al., 2000; Tole et al., 2000; Bai et al., 2002; Motoyama et al., 2003). In the telencephalon, Gli3A is dispensable for global DV patterning, as judged by the absence of telencephalic defects in $Gli3^{\Delta 699/\Delta 699}$ fetuses (present study). By contrast, Gli3R is a major player in telencephalic DV patterning, being essential for both the specification of dorsal fates and the repression of ventral fates (Theil et al., 1999; Tole et al., 2000; Aoto et al., 2002; Rallu et al., 2002; Kuschel et al., 2003). The function of cilia in Gli3R production is thus of prime importance in this process.

The last decade has revealed multiple functions for primary cilia, acting as cellular antennae in sensory perception and signaling. In this context, it is essential to understand how the cilium controls each developmental process. In particular, the developing telencephalon is under the influence of several signaling pathways emanating from different organizing centers. Our findings help to clarify how primary cilia constrain telencephalic morphogenesis by allowing Gli3R production and hence regulating downstream targets of this transcription factor. Moreover, the frequent observation of encephalocoele and the occurrence of OB agenesis in cases of MKS (Ahdab-Barmada and Claassen, 1990; Baala et al., 2007; Khaddour et al., 2007; Sharma et al., 2008) make our findings highly relevant for the physiopathology of this disease.

Acknowledgements

We thank Dr Isabel Le Disquet (electron microscopy platform of the IFR 83, UPMC University Paris 06) and Dr Alain Schmitt (electron microscopy platform of the Institut Cochin CNRS-UMR 8104) for their help with scanning and transmission electron microscopy analyses, respectively; the imaging and animal facilities of the IFR 83 for technical assistance; François Giudicelli, Christine Vesque, Sonia Garel, Jamilé Hazan and Margaret Buckingham for their comments on the manuscript and helpful discussions; Tamara Caspary for providing anti-Arl13b antibody; and Genentech for providing the anti-Gli3 antibody. This work was supported by the Centre National de la Recherche Scientifique; Institut National pour la Santé et la Recherche Médicale; UPMC University Paris 06; Agence Nationale pour la Recherche (project ANR-MRAR-07-Fetalciliopathies); Association pour la Recherche sur le Cancer; the Deutsche Forschung Gemeinschaft (through SFB590 and 612 to U.R.) and the French Ministry of Higher Education and Research (to L.B.).

Competing interests statement

The authors declare no competing financial interests.

Supplementary material

Supplementary material for this article is available at
http://dev.biologists.org/lookup/suppl/doi:10.1242/dev.059808/-/DC1

References

Ahdab-Barmada, M. and Claassen, D. (1990). A distinctive triad of malformations of the central nervous system in the Meckel-Gruber syndrome. *J. Neuropathol. Exp. Neurol.* **49**, 610-620.

Anchan, R. M., Drake, D. P., Haines, C. F., Gerwe, E. A. and LaMantia, A. S. (1997). Disruption of local retinoid-mediated gene expression accompanies abnormal development in the mammalian olfactory pathway. *J. Comp. Neurol.* **379**, 171-184.

Anselme, I., Laclef, C., Lanaud, M., Ruther, U. and Schneider-Maunoury, S. (2007). Defects in brain patterning and head morphogenesis in the mouse mutant Fused toes. *Dev. Biol.* **304**, 208-220.

Aoto, K., Nishimura, T., Eto, K. and Motoyama, J. (2002). Mouse GLI3 regulates Fgf8 expression and apoptosis in the developing neural tube, face, and limb bud. *Dev. Biol.* **251**, 320-332.

Arts, H. H., Doherty, D., van Beersum, S. E., Parisi, M. A., Letteboer, S. J., Gorden, N. T., Peters, T. A., Marker, T., Voesenek, K., Kartono, A. et al. (2007). Mutations in the gene encoding the basal body protein RPGRIP1L, a nephrocystin-4 interactor, cause Joubert syndrome. *Nat. Genet.* **39**, 882-888.

Baala, L., Audollent, S., Martinovic, J., Ozilou, C., Babron, M. C., Sivanandamoorthy, S., Saunier, S., Salomon, R., Gonzales, M., Rattenberry, E. et al. (2007). Pleiotropic effects of CEP290 (NPHP6) mutations extend to Meckel syndrome. *Am. J. Hum. Genet.* **81**, 170-179.

Badano, J. L., Mitsuma, N., Beales, P. L. and Katsanis, N. (2006). The ciliopathies: an emerging class of human genetic disorders. *Annu. Rev. Genomics Hum. Genet.* **7**, 125-148.

Bai, C. B., Auerbach, W., Lee, J. S., Stephen, D. and Joyner, A. L. (2002). Gli2, but not Gli1, is required for initial Shh signaling and ectopic activation of the Shh pathway. *Development* **129**, 4753-4761.

Bai, C. B., Stephen, D. and Joyner, A. L. (2004). All mouse ventral spinal cord patterning by hedgehog is Gli dependent and involves an activator function of Gli3. *Dev. Cell* **6**, 103-115.

Balmer, C. W. and LaMantia, A. S. (2004). Loss of Gli3 and Shh function disrupts olfactory axon trajectories. *J. Comp. Neurol.* **472**, 292-307.

Balmer, C. W. and LaMantia, A. S. (2005). Noses and neurons: induction, morphogenesis, and neuronal differentiation in the peripheral olfactory pathway. *Dev. Dyn.* **234**, 464-481.

Bishop, K. M., Garel, S., Nakagawa, Y., Rubenstein, J. L. and O'Leary, D. D. (2003). Emx1 and Emx2 cooperate to regulate cortical size, lamination, neuronal differentiation, development of cortical efferents, and thalamocortical pathfinding. *J. Comp. Neurol.* **457**, 345-360.

Blanchart, A., De Carlos, J. A. and Lopez-Mascaraque, L. (2006). Time frame of mitral cell development in the mice olfactory bulb. *J. Comp. Neurol.* **496**, 529-543.

Böse, J., Grotewold, L. and Rüther, U. (2002). Pallister-Hall syndrome phenotype in mice mutant for Gli3. *Hum. Mol. Genet.* **11**, 1129-1135.

Brill, M. S., Ninkovic, J., Winpenny, E., Hodge, R. D., Ozen, I., Yang, R., Lepier, A., Gascon, S., Erdelyi, F., Szabo, G. et al. (2009). Adult generation of glutamatergic olfactory bulb interneurons. *Nat. Neurosci.* **12**, 1524-1533.

Büscher, D. and Rüther, U. (1998). Expression profile of Gli family members and Shh in normal and mutant mouse limb development. *Dev. Dyn.* **211**, 88-96.

Caspary, T., Larkins, C. E. and Anderson, K. V. (2007). The graded response to Sonic hedgehog depends on cilia architecture. *Dev. Cell* **12**, 767-778.

Chizhikov, V. V., Davenport, J., Zhang, Q., Shih, E. K., Cabello, O. A., Fuchs, J. L., Yoder, B. K. and Millen, K. J. (2007). Cilia proteins control cerebellar morphogenesis by promoting expansion of the granule progenitor pool. *J. Neurosci.* **27**, 9780-9789.

Cobos, I., Shimamura, K., Rubenstein, J. L., Martinez, S. and Puelles, L. (2001). Fate map of the avian anterior forebrain at the four-somite stage, based on the analysis of quail-chick chimeras. *Dev. Biol.* **239**, 46-67.

Cortellino, S., Wang, C., Wang, B., Bassi, M. R., Caretti, E., Champeval, D., Calmont, A., Jarnik, M., Burch, J., Zaret, K. S. et al. (2009). Defective ciliogenesis, embryonic lethality and severe impairment of the Sonic Hedgehog pathway caused by inactivation of the mouse complex A intraflagellar transport gene Ift122/Wdr10, partially overlapping with the DNA repair gene Med1/Mbd4. *Dev. Biol.* **325**, 225-237.

Dellovade, T. L., Pfaff, D. W. and Schwanzel-Fukuda, M. (1998). Olfactory bulb development is altered in small-eye (Sey) mice. *J. Comp. Neurol.* **402**, 402-418.

Delous, M., Baala, L., Salomon, R., Laclef, C., Vierkotten, J., Tory, K., Golzio, C., Lacoste, T., Besse, L., Ozilou, C. et al. (2007). The ciliary gene RPGRIP1L is mutated in cerebello-oculo-renal syndrome (Joubert syndrome type B) and Meckel syndrome. *Nat. Genet.* **39**, 875-881.

Ding, Q., Motoyama, J., Gasca, S., Mo, R., Sasaki, H., Rossant, J. and Hui, C. C. (1998). Diminished Sonic hedgehog signaling and lack of floor plate differentiation in Gli2 mutant mice. *Development* **125**, 2533-2543.

Eggenschwiler, J. T. and Anderson, K. V. (2007). Cilia and developmental signaling. *Annu. Rev. Cell Dev. Biol.* **23**, 345-373.

Englund, C., Fink, A., Lau, C., Pham, D., Daza, R. A., Bulfone, A., Kowalczyk, T. and Hevner, R. F. (2005). Pax6, Tbr2, and Tbr1 are expressed sequentially by radial glia, intermediate progenitor cells, and postmitotic neurons in developing neocortex. *J. Neurosci.* **25**, 247-251.

Faedo, A., Ficara, F., Ghiani, M., Aiuti, A., Rubenstein, J. L. and Bulfone, A. (2002). Developmental expression of the T-box transcription factor T-bet/Tbx21 during mouse embryogenesis. *Mech. Dev.* **116**, 157-160.

Feng, W., Simoes-de-Souza, F., Finger, T. E., Restrepo, D. and Williams, T. (2009). Disorganized olfactory bulb lamination in mice deficient for transcription factor AP-2epsilon. *Mol. Cell. Neurosci.* **42**, 161-171.

Fukuchi-Shimogori, T. and Grove, E. A. (2003). Emx2 patterns the neocortex by regulating FGF positional signaling. *Nat. Neurosci.* **6**, 825-831.

Garel, S., Huffman, K. J. and Rubenstein, J. L. (2003). Molecular regionalization of the neocortex is disrupted in Fgf8 hypomorphic mutants. *Development* **130**, 1903-1914.
Gerdes, J. M. and Katsanis, N. (2008). Ciliary function and Wnt signal modulation. *Curr. Top. Dev. Biol.* **85**, 175-195.
Gerdes, J. M., Davis, E. E. and Katsanis, N. (2009). The vertebrate primary cilium in development, homeostasis, and disease. *Cell* **137**, 32-45.
Gong, Q. and Shipley, M. T. (1995). Evidence that pioneer olfactory axons regulate telencephalon cell cycle kinetics to induce the formation of the olfactory bulb. *Neuron* **14**, 91-101.
Gorivodsky, M., Mukhopadhyay, M., Wilsch-Braeuninger, M., Phillips, M., Teufel, A., Kim, C., Malik, N., Huttner, W. and Westphal, H. (2009). Intraflagellar transport protein 172 is essential for primary cilia formation and plays a vital role in patterning the mammalian brain. *Dev. Biol.* **325**, 24-32.
Han, Y. G., Spassky, N., Romaguera-Ros, M., Garcia-Verdugo, J. M., Aguilar, A., Schneider-Maunoury, S. and Alvarez-Buylla, A. (2008). Hedgehog signaling and primary cilia are required for the formation of adult neural stem cells. *Nat. Neurosci.* **11**, 277-284.
Haycraft, C. J., Banizs, B., Aydin-Son, Y., Zhang, Q., Michaud, E. J. and Yoder, B. K. (2005). Gli2 and Gli3 localize to cilia and require the intraflagellar transport protein polaris for processing and function. *PLoS Genet.* **1**, e53.
Hebert, J. M. and Fishell, G. (2008). The genetics of early telencephalon patterning: some assembly required. *Nat. Rev. Neurosci.* **9**, 678-685.
Hebert, J. M., Lin, M., Partanen, J., Rossant, J. and McConnell, S. K. (2003). FGF signaling through FGFR1 is required for olfactory bulb morphogenesis. *Development* **130**, 1101-1111.
Hill, P., Wang, B. and Rüther, U. (2007). The molecular basis of Pallister Hall associated polydactyly. *Hum. Mol. Genet.* **16**, 2089-2096.
Hirata, T., Nakazawa, M., Yoshihara, S., Miyachi, H., Kitamura, K., Yoshihara, Y. and Hibi, M. (2006). Zinc-finger gene Fez in the olfactory sensory neurons regulates development of the olfactory bulb non-cell-autonomously. *Development* **133**, 1433-1443.
Hoover, A. N., Wynkoop, A., Zeng, H., Jia, J., Niswander, L. A. and Liu, A. (2008). C2cd3 is required for cilia formation and Hedgehog signaling in mouse. *Development* **135**, 4049-4058.
Huangfu, D. and Anderson, K. V. (2005). Cilia and Hedgehog responsiveness in the mouse. *Proc. Natl. Acad. Sci. USA* **102**, 11325-11330.
Huangfu, D. and Anderson, K. V. (2006). Signaling from Smo to Ci/Gli: conservation and divergence of Hedgehog pathways from Drosophila to vertebrates. *Development* **133**, 3-14.
Hui, C. C. and Joyner, A. L. (1993). A mouse model of Greig cephalo-polysyndactyly syndrome: the *extra-toes*^{J} mutation contains an intragenic deletion of the *Gli3* gene. *Nat. Genet.* **3**, 241-246.
Jimenez, D., Garcia, C., de Castro, F., Chedotal, A., Sotelo, C., de Carlos, J. A., Valverde, F. and Lopez-Mascaraque, L. (2000). Evidence for intrinsic development of olfactory structures in Pax-6 mutant mice. *J. Comp. Neurol.* **428**, 511-526.
Johnson, D. R. (1967). Extra-toes: anew mutant gene causing multiple abnormalities in the mouse. *J. Embryol. Exp. Morphol.* **17**, 543-581.
Khaddour, R., Smith, U., Baala, L., Martinovic, J., Clavering, D., Shaffiq, R., Ozilou, C., Cullinane, A., Kyttala, M., Shalev, S. et al. (2007). Spectrum of *MKS1* and *MKS3* mutations in Meckel syndrome: a genotype-phenotype correlation. *Hum. Mutat.* **28**, 523-524.
Kuschel, S., Rüther, U. and Theil, T. (2003). A disrupted balance between Bmp/Wnt and Fgf signaling underlies the ventralization of the Gli3 mutant telencephalon. *Dev. Biol.* **260**, 484-495.
LaMantia, A. S. (1999). Forebrain induction, retinoic acid, and vulnerability to schizophrenia: insights from molecular and genetic analysis in developing mice. *Biol. Psychiatry* **46**, 19-30.
Liu, A., Wang, B. and Niswander, L. A. (2005). Mouse intraflagellar transport proteins regulate both the activator and repressor functions of Gli transcription factors. *Development* **132**, 3103-3111.
Long, J. E., Garel, S., Depew, M. J., Tobet, S. and Rubenstein, J. L. (2003). DLX5 regulates development of peripheral and central components of the olfactory system. *J. Neurosci.* **23**, 568-578.
Marin, O. and Rubenstein, J. L. (2003). Cell migration in the forebrain. *Annu. Rev. Neurosci.* **26**, 441-483.
Marshall, W. F. (2008). Basal bodies platforms for building cilia. *Curr. Top. Dev. Biol.* **85**, 1-22.
May, S. R., Ashique, A. M., Karlen, M., Wang, B., Shen, Y., Zarbalis, K., Reiter, J., Ericson, J. and Peterson, A. S. (2005). Loss of the retrograde motor for IFT disrupts localization of Smo to cilia and prevents the expression of both activator and repressor functions of Gli. *Dev. Biol.* **287**, 378-389.
Meyer, N. P. and Roelink, H. (2003). The amino-terminal region of Gli3 antagonizes the Shh response and acts in dorsoventral fate specification in the developing spinal cord. *Dev. Biol.* **257**, 343-355.
Meyers, E. N., Lewandoski, M. and Martin, G. R. (1998). An Fgf8 mutant allelic series generated by Cre- and Flp-mediated recombination. *Nat. Genet.* **18**, 136-141.
Motoyama, J., Milenkovic, L., Iwama, M., Shikata, Y., Scott, M. P. and Hui, C. C. (2003). Differential requirement for Gli2 and Gli3 in ventral neural cell fate specification. *Dev. Biol.* **259**, 150-161.
Neugebauer, J. M., Amack, J. D., Peterson, A. G., Bisgrove, B. W. and Yost, H. J. (2009). FGF signalling during embryo development regulates cilia length in diverse epithelia. *Nature* **458**, 651-654.
Park, H. L., Bai, C., Platt, K. A., Matise, M. P., Beeghly, A., Hui, C. C., Nakashima, M. and Joyner, A. L. (2000). Mouse Gli1 mutants are viable but have defects in SHH signaling in combination with a Gli2 mutation. *Development* **127**, 1593-1605.
Rallu, M., Machold, R., Gaiano, N., Corbin, J. G., McMahon, A. P. and Fishell, G. (2002). Dorsoventral patterning is established in the telencephalon of mutants lacking both Gli3 and Hedgehog signaling. *Development* **129**, 4963-4974.
Rosenbaum, J. L. and Witman, G. B. (2002). Intraflagellar transport. *Nat. Rev. Mol. Cell Biol.* **3**, 813-825.
Salic, A. and Mitchison, T. J. (2008). A chemical method for fast and sensitive detection of DNA synthesis in vivo. *Proc. Natl. Acad. Sci. USA* **105**, 2415-2420.
Sharma, N., Berbari, N. F. and Yoder, B. K. (2008). Ciliary dysfunction in developmental abnormalities and diseases. *Curr. Top. Dev. Biol.* **85**, 371-427.
Spassky, N., Han, Y. G., Aguilar, A., Strehl, L., Besse, L., Laclef, C., Ros, M. R., Garcia-Verdugo, J. M. and Alvarez-Buylla, A. (2008). Primary cilia are required for cerebellar development and Shh-dependent expansion of progenitor pool. *Dev. Biol.* **317**, 246-259.
St John, J. A., Clarris, H. J., McKeown, S., Royal, S. and Key, B. (2003). Sorting and convergence of primary olfactory axons are independent of the olfactory bulb. *J. Comp. Neurol.* **464**, 131-140.
Stenman, J., Toresson, H. and Campbell, K. (2003). Identification of two distinct progenitor populations in the lateral ganglionic eminence: implications for striatal and olfactory bulb neurogenesis. *J. Neurosci.* **23**, 167-174.
Stottmann, R. W., Tran, P. V., Turbe-Doan, A. and Beier, D. R. (2009). Ttc21b is required to restrict sonic hedgehog activity in the developing mouse forebrain. *Dev. Biol.* **335**, 166-178.
Stout, R. P. and Graziadei, P. P. (1980). Influence of the olfactory placode on the development of the brain in Xenopus laevis (Daudin). I. Axonal growth and connections of the transplanted olfactory placode. *Neuroscience* **5**, 2175-2186.
Tempe, D., Casas, M., Karaz, S., Blanchet-Tournier, M. F. and Concordet, J. P. (2006). Multisite protein kinase A and glycogen synthase kinase 3beta phosphorylation leads to Gli3 ubiquitination by SCFbetaTrCP. *Mol. Cell. Biol.* **26**, 4316-4326.
Theil, T., Alvarez-Bolado, G., Walter, A. and Rüther, U. (1999). Gli3 is required for Emx gene expression during dorsal telencephalon development. *Development* **126**, 3561-3571.
Tole, S., Ragsdale, C. W. and Grove, E. A. (2000). Dorsoventral patterning of the telencephalon is disrupted in the mouse mutant extra-toes(J). *Dev. Biol.* **217**, 254-265.
Tran, P. V., Haycraft, C. J., Besschetnova, T. Y., Turbe-Doan, A., Stottmann, R. W., Herron, B. J., Chesebro, A. L., Qiu, H., Scherz, P. J., Shah, J. V. et al. (2008). THM1 negatively modulates mouse sonic hedgehog signal transduction and affects retrograde intraflagellar transport in cilia. *Nat. Genet.* **40**, 403-410.
Vierkotten, J., Dildrop, R., Peters, T., Wang, B. and Rüther, U. (2007). Ftm is a novel basal body protein of cilia involved in Shh signalling. *Development* **134**, 2569-2577.
Wang, B., Fallon, J. F. and Beachy, P. A. (2000). Hedgehog-regulated processing of Gli3 produces an anterior/posterior repressor gradient in the developing vertebrate limb. *Cell* **100**, 423-434.
Watanabe, Y., Inoue, K., Okuyama-Yamamoto, A., Nakai, N., Nakatani, J., Nibu, K., Sato, N., Iiboshi, Y., Yusa, K., Kondoh, G. et al. (2009). Fezf1 is required for penetration of the basal lamina by olfactory axons to promote olfactory development. *J. Comp. Neurol.* **515**, 565-584.
Whitesides, J. G., 3rd and LaMantia, A. S. (1996). Differential adhesion and the initial assembly of the mammalian olfactory nerve. *J. Comp. Neurol.* **373**, 240-254.
Willaredt, M. A., Hasenpusch-Theil, K., Gardner, H. A., Kitanovic, I., Hirschfeld-Warneken, V. C., Gojak, C. P., Gorgas, K., Bradford, C. L., Spatz, J., Wolfl, S. et al. (2008). A crucial role for primary cilia in cortical morphogenesis. *J. Neurosci.* **28**, 12887-12900.
Wong, S. Y. and Reiter, J. F. (2008). The primary cilium at the crossroads of mammalian hedgehog signaling. *Curr. Top. Dev. Biol.* **85**, 225-260.
Yun, K., Potter, S. and Rubenstein, J. L. (2001). Gsh2 and Pax6 play complementary roles in dorsoventral patterning of the mammalian telencephalon. *Development* **128**, 193-205.